NANO LETTERS

Letter

pubs.acs.org/NanoLett

Subwavelength Lattice Optics by Evolutionary Design

Mark D. Huntington,[†] Lincoln J. Lauhon,[†] and Teri W. Odom*[,†,‡]

[†]Department of Materials Science and Engineering, Northwestern University, Evanston, Illinois 60208, United States

[‡]Department of Chemistry, Northwestern University, Evanston, Illinois 60208, United States

Supporting Information

ABSTRACT: This paper describes a new class of structured optical materials—lattice opto-materials—that can manipulate the flow of visible light into a wide range of three-dimensional profiles using evolutionary design principles. Lattice opto-materials are based on the discretization of a surface into a two-dimensional (2D) subwavelength lattice whose individual lattice sites can be controlled to achieve a programmed optical response. To access a desired optical property, we designed a lattice evolutionary algorithm that includes and optimizes contributions from every element in the lattice. Lattice opto-materials can exhibit simple properties, such as on- and off-axis focusing, and can also concentrate light into multiple, discrete spots. We expanded the unit cell shapes of the lattice to achieve distinct, polarization-dependent optical responses from the same 2D patterned substrate. Finally, these lattice opto-materials can also be combined into architectures that resemble a new type of compound flat lens.

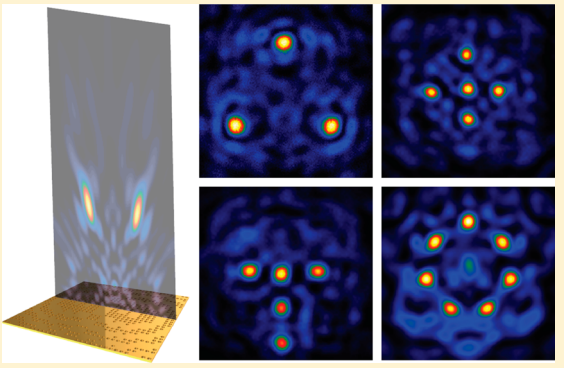

KEYWORDS: *metasurfaces, flat lenses, optics, nanomaterials, nanoholes, evolutionary design*

The discovery of new materials has been accelerated by computational methods that can screen the constituent elements for a desired application.[1−3] In principle, such tools could be extended to artificially structured materials such as metamaterials and metasurfaces, where each subwavelength unit could act as a design variable.[4] Instead, these designs have relied on analytical descriptions from far-field optics that do not consider the unique near-field distributions of the unit shapes or fabrication challenges involved in creating these structures.[5−7] For simple structures with a small number of design variables, iterative optimization methods have been used to screen for a specific physical property.[8,9] For more complex structures, however, solving the inverse problem computationally has remained an elusive challenge[10] because there are nearly an infinite number of design configurations that could produce the anomalous optical properties.[10−12] Evolutionary design methods have been successfully used to predict metamaterial unit cell shapes that operate at terahertz frequencies because the constituent materials are not lossy;[13,14] however, these strategies encounter challenges at optical frequencies. Therefore, a key problem in achieving a desired far-field optical response from metallic nanostructures at visible wavelengths is accounting for losses at the plasma frequency,[15,16] which requires a fine (several nanometers) computational grid, and hence large computation times, to simulate 3D optical profiles.

Here, we report a bottom-up strategy that can manipulate the flow of visible light into distinct profiles in 3D space. Our method exploits a custom-built evolutionary algorithm to optimize a new class of artificial materials—lattice opto-materials—based on discretization of a plasmonic film into a 2D subwavelength lattice of holes. This approach to the inverse problem can screen a large number of candidate solutions quickly by casting nanoscale optical elements on a 2D grid and then adding the complex electric fields from each lattice position. Lattice opto-materials can support properties that are simple, such as focusing light on- or off-axis, as well as those that are more complex, including concentrating light into numerous distinct regions of space. In addition, dynamic tuning of the 3D light profiles can be realized by changing the shape of the lattice units so that they are sensitive to the polarization of light. Finally, lattice opto-materials can be combined into hierarchical architectures not yet explored by existing flat optics, such as planar compound lenses.

To establish our design approach at visible wavelengths, we first tested lattice opto-materials that could manipulate light in 3D using a single phase element: a circular hole. We arranged nanoholes in a metal film on a 2D grid (a_0 = 300 nm) with a 10 μm × 10 μm footprint. In this design, there are 33 × 33 elements, or 2^{1089} total possible arrangements of lattice units (open hole or closed hole) that represent unique optical focusing profiles. Analyzing all unit combinations for a targeted response is not possible; therefore, we developed a lattice evolution algorithm (LEA) that could efficiently identify the optimal lattice opto-material for a desired far-field characteristic (Figure 1). LEA is similar to other evolutionary algorithms such as genetic algorithms, where the solution is found by sequentially evolving a population of potential solutions to

Received: October 22, 2014
Published: November 7, 2014

   dx.doi.org/10.1021/nl5040573 | *Nano Lett.* 2014, 14, 7195−7200

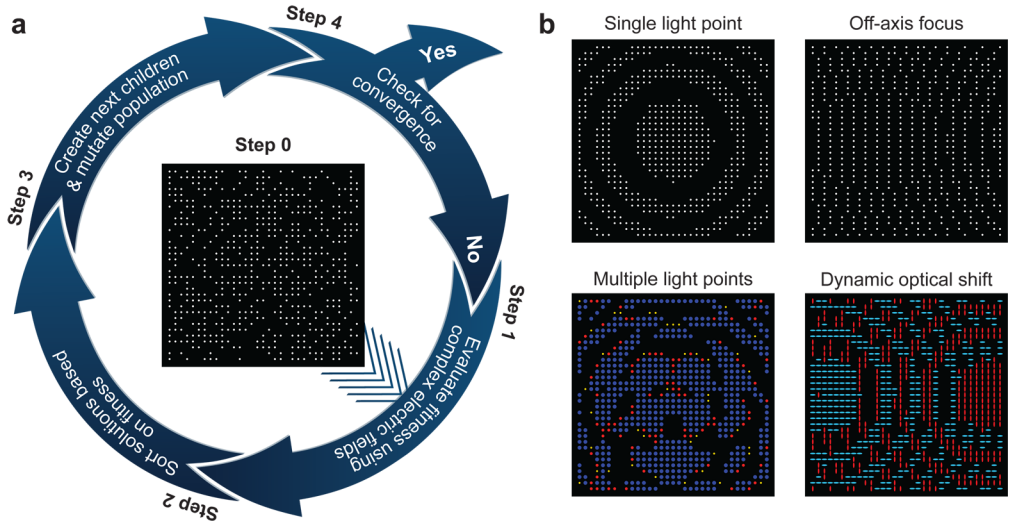

Figure 1. Evolutionary design methods can be used to design lattice opto-materials with unique focal properties. (a) Scheme depicting the four steps involved in the LEA. Step 0 is a randomly arranged lattice. After the algorithm converges, final lattice designs are created. (b) Four representative lattice structures that demonstrate the types of lattice opto-materials that the LEA can produce by changing the fitness function.

maximize a fitness function, except here an optimized optical response is formed from nanostructures constrained to a 2D grid (lattice).

Our LEA can be summarized in four cyclic steps (Figure 1a); details are in the Supporting Information. To initialize the LEA, we created a 600-member "population" of candidate lattice opto-materials with randomly generated arrangements of holes. Besides fabrication considerations, one important advantage of constraining the nanoscale elements to a 2D lattice is that lattice opto-materials can be represented by a binary array and first optimized *in silico*. The configuration for each lattice opto-material was represented by "DNA" (step 0), a large binary array (1089 elements), where for the case of a single phase element, an open hole is denoted as a 1 and a closed hole as a 0 (Supporting Information Figure S1). The viability of each member was evaluated using a fitness function (step 1), which for a lattice opto-material designed to focus light into single intensity point can be defined as

$$F(f_d) = \frac{I}{(f_d - d) + c} \quad (1)$$

where F is the fitness parameter, I is the intensity at the desired focal point, d is the location of the maximum intensity, f_d is the focal point, and c is a constant. We evaluated F by calculating electric field intensity distributions in the far-field profile by adding complex field contributions from each nanohole in the DNA string. The electric-field components can be calculated by different methods. For LEA, we used both point-source simulations[17] (Supporting Information Figures S2−S3) based on the Huygens−Fresnel principle[18] and finite-difference time-domain (FDTD) simulations (Supporting Information Figure S4) to generate the fields. Point-source simulations required less overall simulation times and were first used to validate our approach; however, they cannot describe nanoscale elements with different phases. Therefore, we selected the simulation method appropriate for the constituent elements composing the lattice opto-material.

For example, lattice opto-materials with single-phase elements (i.e., circular holes of the same size), were simulated using point-source methods, and more complex lattice opto-materials having two or more phase units (i.e., holes with different sizes) required FDTD methods. To increase the efficiency of the LEA, we first stored all of the complex field information in memory. Then, we could calculate the 3D optical profiles by adding different combinations of complex fields instead of simulating the entire field for each lattice opto-material structure, which decreased computation times by a factor of ca. 10^5 compared to simulating the entire structure in FDTD.

In step 2, the population was then sorted by fitness, and a new generation of the population was created by combining the DNA of the members of the previous generation (step 3). In the combination process, preference was given to members of the population with higher fitness by using the roulette wheel selection method.[19] This cycle continued until the LEA reached a convergence condition (step 4), which we designated as when the fittest member in the population did not change for 30 generations (Supporting Information Figure S5). After optimizing the parameters for the LEA, such as population size and mutation rate, we could design a lattice opto-material for a single design criterion (e.g., single focal point) in ∼210 generations with an overall computation time of ∼0.45 CPU hours (27 min). One key advantage of using a LEA to design lattice opto-materials is that different 3D optical profiles—from the same finite grid—are possible simply by redefining F.

Figure 1b shows calculated final nanohole configurations of four representative lattice opto-materials produced by four different fitness functions. As a proof-of-concept lattice opto-material, we solved and fabricated a nanohole arrangement that could focus light into a single position in the center of the x−y plane at different focal distances (Supporting Information Figure S6). The evolutionary process is summarized in the Supporting Information Video S1. With the same nanohole size, lattice spacing, and overall footprint, the calculated focal distances could be tuned from 3 to 14 μm with ±50 nm precision (Supporting Information Figure S7−S8). We then fabricated lattice opto-materials in optically opaque (180 nm thick) gold films using focused ion beam (FIB) milling to drill holes (diameter, d = 150 nm) (Supporting Information Figure S9) and mapped the transmitted 3D optical profile using confocal scanning optical microscopy (Supporting Informa-

dx.doi.org/10.1021/nl5040573 | *Nano Lett.* 2014, 14, 7195−7200

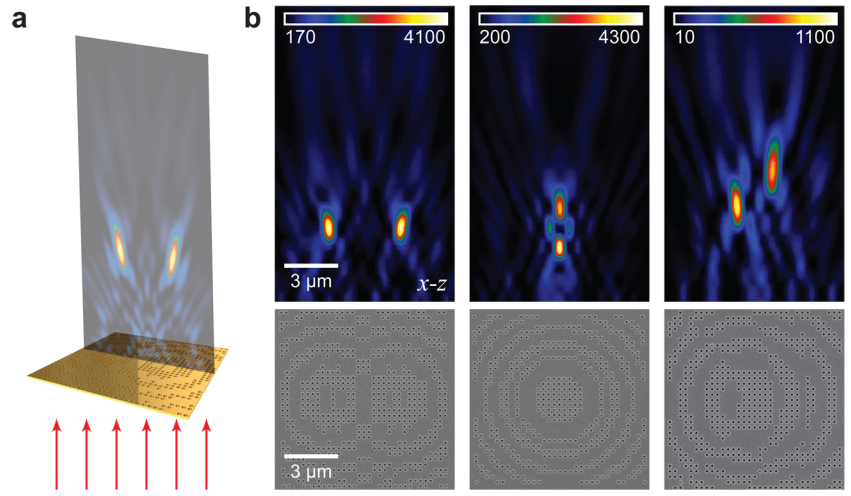

Figure 2. Lattice opto-materials can concentrate light into two focal points in the optical far-field. (a) Scheme of experimental setup, where collimated laser light (red arrows, λ = 690 nm) is incident on the lattice opto-material. The far-field profile through the center of the lattice opto-material (x = 0, y = 0) was measured using confocal optical microscopy. (b) Scanning electron microscopy (SEM) images of lattice opto-material structures (lower) and confocal microscopy data (upper, λ = 690 nm) for lattice opto-materials with two focal points at f_d = 4 μm, x = ±2 μm, y = 0 (left); f_d = 3, 5 μm, x = 0, y = 0 (middle); and f_d = 5, 7 μm, x = ±1 μm, y = 0 (right).

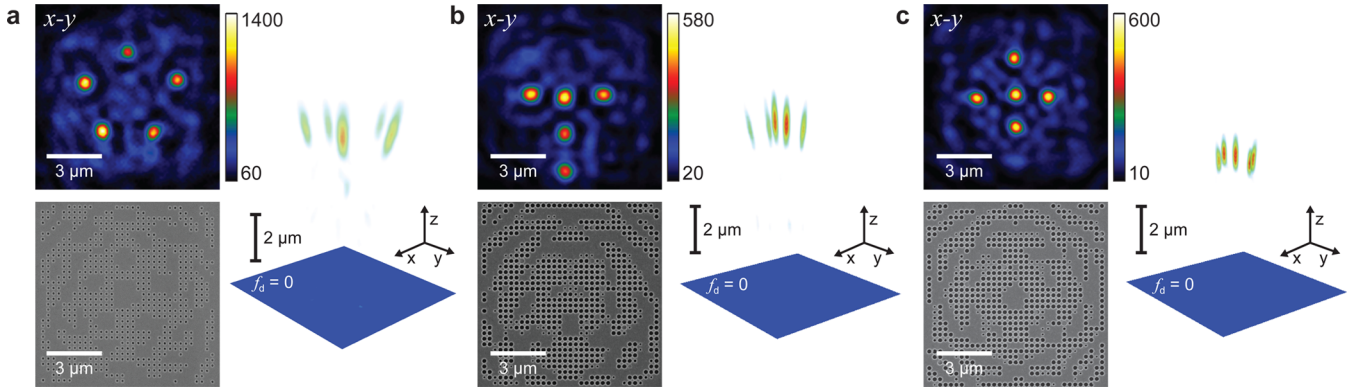

Figure 3. Lattice opto-materials can generate arbitrary light profiles in 3D. SEM images of lattice opto-material structures (lower), 2D confocal microscopy slices at the focal plane (upper, λ = 690 nm), and 3D volume profile (right). (a) Five focal points at f_d = 7 μm from single phase elements. All focal points had a constant distance (r = 3 μm) from the center of the lattice. (b) Five focal points at f_d = 7 μm from three phase units in a "T" shape with 1-μm separation between points. (c) Five focal points at f_d = 5 μm from three phase units in an "X" shape with 1-μm separation between points.

tion). Not surprisingly, and as validation of the LEA, the nanohole configurations for a single focal point were similar to that of a Fresnel zone plate.[20] The measured lattice opto-materials could also be designed to operate at different wavelengths but at the same focal distance (Supporting Information Figure S10).

As described earlier, a distinct advantage of lattice opto-materials designed by LEA, beyond what can be produced by finite arrays of ordered or disordered nanoholes, is their ability to produce a large range of different 3D optical profiles simply by specifying F. Figure 2a highlights a scheme of the transformation of a plane-wave into two focal spots, which requires a generalization of F to

$$F(F_i) = \sum_i \frac{F_i(f_d^i)}{\max(F_i(f_d^i))} \quad (2)$$

where i represents each light spot and ranges from 1 to the total number of intensity points in the design problem. Note that the distance (f_d^i) is now a 3D vector from the center of the lattice (Supporting Information Figure S11). The main challenge in optimization problems is to find a solution that balances among all the objectives. In contrast to other computational approaches such as Monte Carlo,[21] evolutionary algorithms are efficient at solving problems with two or more criteria.[22] Supporting Information Figure S12 summarizes the ability of LEA to solve a two-objective problem by designing a lattice opto-material with two focal points at the same focal distance ($\|f_d^1\| = \|f_d^2\|$). The evolutionary process is shown in the Supporting Information Video S2. Figure 2b shows that experimentally, visible light can be concentrated into two foci with similar intensities. Lattice opto-materials could also concentrate light at different distances above the surface (Figure 2c).

Figure 3 shows lattice opto-materials designed to concentrate light at five distinct locations. For simplicity in imaging, we chose all focal distances to be at the same height. We tested prime numbers (Supporting Information Figure S13–S14) to illustrate that these solutions were not a result of diffraction from the Talbot effect.[23] Figure 3a demonstrates that a lattice opto-material with a single phase element could create a unique

dx.doi.org/10.1021/nl5040573 | Nano Lett. 2014, 14, 7195–7200

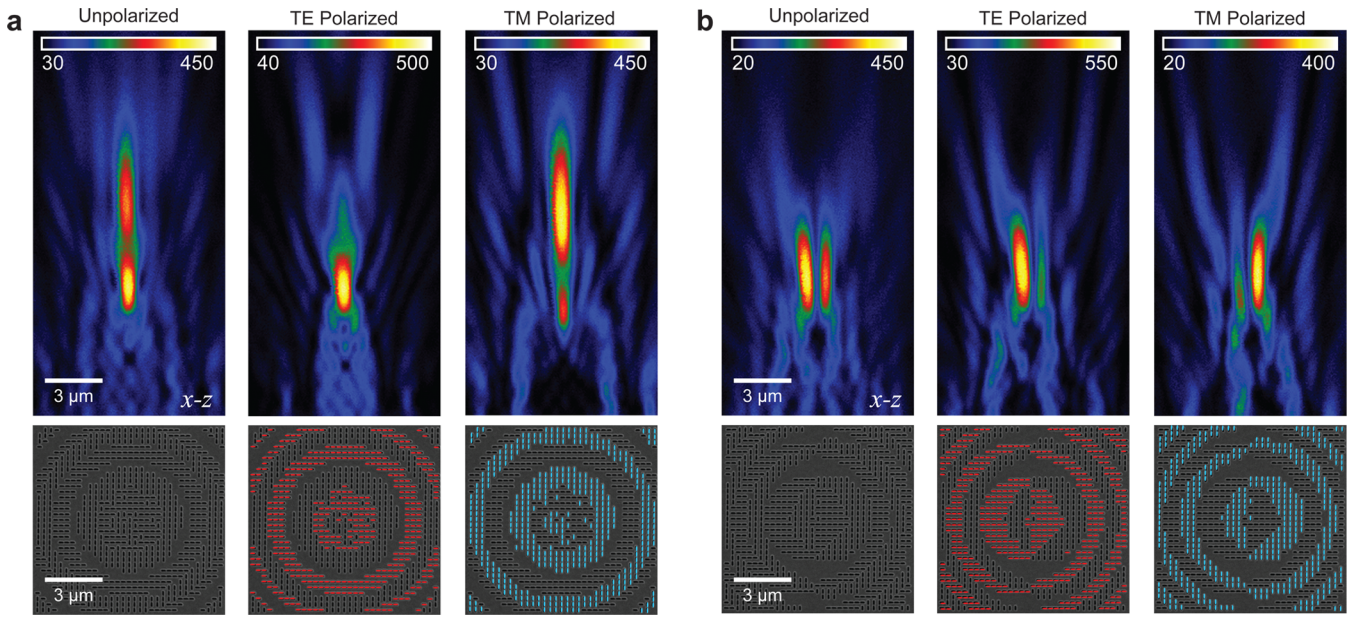

Figure 4. Lattice opto-materials can exhibit dynamic optical profiles based on polarization of incident light. Polarization-sensitive lattice opto-materials with (a) dynamic focal depth (f_d = 7 μm and f_d = 10 μm, x = 0, y = 0) and (b) dynamic focal shift (f_d = 7 μm and x = ±0.5 μm, y = 0). SEM images of lattice opto-material structures (lower) and confocal microscopy data (upper, λ = 770 nm). The polarization-sensitive lattice opto-materials were measured with unpolarized, TE, and TM polarized light. Holes active under TE and TM polarization are indicated in red and blue, respectively. Under unpolarized light, all holes transmitted (left images in (a), (b)).

3D optical profile. In this case, the five light spots were in a ring-structure with no central spot. For metasurfaces, phase control over adjacent structures is critical to observe anomalous far-field optical properties.[24] In contrast, lattice opto-materials constructed from single-phase elements can generate different optical profiles without phase constraints on the neighboring lattice elements.

To increase the overall transmission and diffraction efficiency, we also designed lattice opto-materials having more than one type of phase element. The binary representation of open/closed holes used in LEA allows for arbitrarily large numbers of unit types without a significant increase in the array size. For example, 2, 4, or 8 binary numbers could represent 4, 16, or 128 different element types. Although we could have selected any geometrical structure for phase elements, including v-shaped nanoantennas typically used in metasurfaces,[11,12,20] we chose three circular holes with different sizes (d = 100, 150, 200 nm) because they are easy to fabricate by FIB (Supporting Information Figure S7). To represent the different hole sizes in the LEA, we added a second binary digit to the DNA array so that each position on the 2D grid now had one of four values: 00 (closed hole), 01 (d = 100 nm), 10 (d = 150 nm), or 11 (d = 200 nm). For these phase elements, we needed to consider the different field distributions for the different hole sizes, and thus the complex electric and magnetic fields were modeled by FDTD simulations. Interestingly, although our lattice opto-materials are made of optically thick gold, the calculated transmission efficiency can be up to 20% (Supporting Information Figures S15−S16), over twice that of any reported metasurface at visible wavelengths.[11,25]

Figure 3b−c indictates that lattice opto-materials with three phase elements (i.e., three different hole sizes) can also manipulate light into distinct "T" and "X" shapes. Although lattice optics with single phase units could also produce these shapes, the inclusion of the two additional elements improved the efficiency. For example, we measured a diffraction efficiency of ∼74% for the T-shaped lattice opto-material, determined by the ratio of light intensity at the focal points to the transmission at the lattice plane, while five light spots from single phase elements had a diffraction efficiency of 55%. The measured profiles of the lattice opto-materials with multiple phase elements matched well with simulated profiles (Supporting Information Figure S17), indicating that FDTD can be used to predict the far-field[26] profiles accurately. These examples of lattice opto-materials highlight the power of LEA to design flat optics that can transform an incident plane wave into discrete regions of light. Moreover, the LEA can produce many different 3D optical profiles depending on how the fitness function F is defined. For example, F could be developed to manipulate incident light into continuous structures, although here we have focused primarily on droplets of light.

To demonstrate that the LEA could be used with nanoscale elements with different shapes, we tested unit cells with anisotropic shapes sensitive to polarized light.[17,27−29] We focused on elliptical holes to design static lattice opto-materials with dynamic properties (Figure 4). Anisotropic apertures in plasmonic films can transmit up to 100 times more light when the polarization is perpendicular to the major axis of the hole.[17,26] Therefore, by modulating polarization, we could effectively "close" nanoholes in the array. We represented the orientation of the major axis of the ellipse by assigning each position in the 2D grid as one of three values: 00 (closed ellipse), 01 (vertical ellipse), or 10 (horizontal ellipse). Because changing the hole shape from circular to elliptical (r_{minor} = 70 nm, r_{major} = 250 nm) caused the EOT resonance to red-shift from 690 to 770 nm (Supporting Information Figure S18), the optical profiles were simulated and measured with λ = 770 nm. Figure 4a illustrates how light can be focused to different distances along the optical axis, where transverse electric (TE) polarized light was focused at 7 μm above the lattice plane and transverse magnetic (TE) polarized light to 10 μm. Thus, the same lattice structure can produce two independent focusing

dx.doi.org/10.1021/nl5040573 | Nano Lett. 2014, 14, 7195−7200

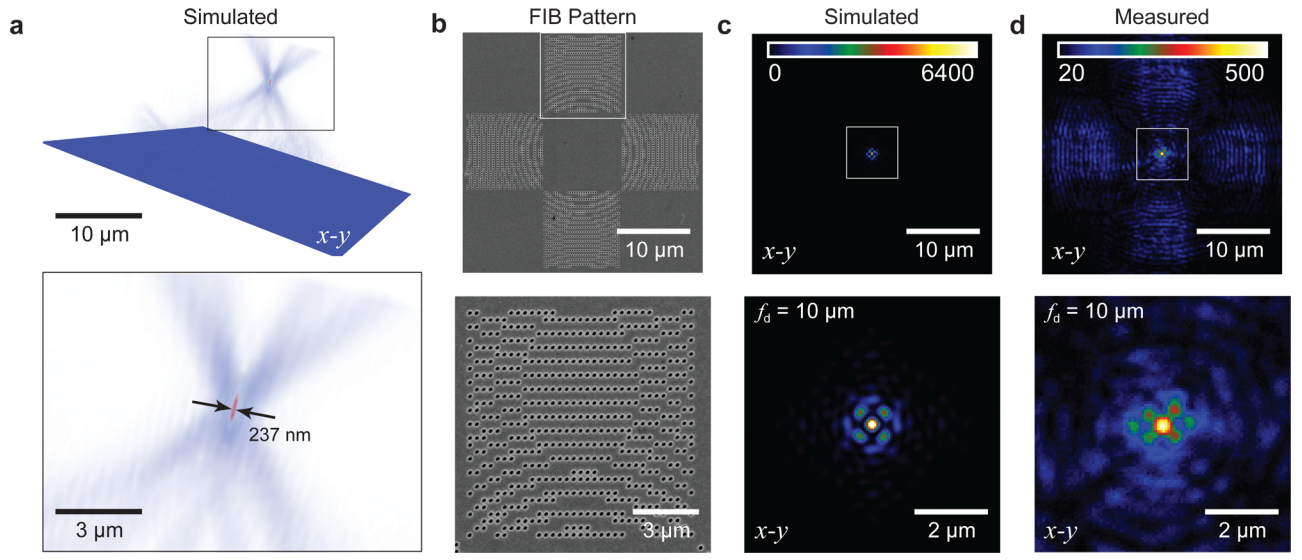

Figure 5. Compound lattice opto-materials can achieve smaller focal points than single lenses. (a) Simulated 3D data of the interference of four lattice opto-materials at λ = 690 nm and n = 1.5. (b) SEM images of compound lattice opto-material structures fabricated by FIB milling in a 180 nm thick gold film. (c) Simulated and (d) confocal microscopy images (λ = 690 nm, n = 1.5) of x–y cross sections of four interfering lattice opto-materials at the focal distance (f_d = 10 μm).

profiles. Both focal distances are larger than what could be achieved with refractive microlenses of the same footprint.[30] Agreement between measured and simulated results (Supporting Information Figure S19) verified that transmission through individual ellipses could also be represented by point-source simulations.

In addition, we used polarization-sensitive lattice opto-materials to shift laterally (Δx = 1500, 2500, 3000, and 4000 nm) the focused light far away from the center of the lattice (Supporting Information Figure S20). Because the ellipses act as near-field polarization filters, we anticipated there would not be any interference between light transmitted through horizontal and vertical holes. Indeed, unpolarized light resulted in high-intensity points at both focal locations (Figure 4a and Supporting Information Figure S20), which indicates that the light transmitted though horizontal or vertical ellipses acts independently. To establish further that the focal profiles were separate, we designed a polarization-sensitive lattice opto-materials with overlapping focal points (f_d = 7 μm, Δx = 500 nm). Under unpolarized light, we still observed two distinct focal points (Figure 4b), in agreement with simulation (Supporting Information Figure S21).

Finally, for ultimate light management, flat optics need to be integrated into optical systems; however, microlenses and metasurfaces are difficult to combine into compound arrangements because fabrication challenges preclude alignment along the optical axis.[30] Lattice opto-materials overcome this limitation because although their profile is flat, their focal point can be located far off-axis. As a proof-of-concept compound surface lens, we designed lattice opto-materials such that the focusing profiles of four structures overlapped. Each lattice had a single focal point at f_d = 10 μm, shifted 10 μm away from the optical axis (Figure 5). Figure 5a shows simulated results of four lattice optics that focused light to the same location in 3D. The fwhm of the interference spot at the center of the tilted beams was 237 nm, more than three times smaller than the diffraction limit for a single 10-μm lens (fwhm = 752 nm, calculated) at the same height (f_d = 10 μm).

In contrast to the concentric rings that focused light above the center of the lattice (Figure 1b), these lattice opto-materials were composed of arcs of holes so that the light could be directed away from the optical axis (Figure 5b). To realize this compound system, we designed lattice opto-materials to operate in a higher refractive index environment (n = 1.525). As expected from simulation, the measurements showed strong interference with a high-intensity spot where the four beams overlapped (Figure 5c–d). We also tested these lattice opto-material in a bright-field optical microscope using a filtered broadband source (λ = 700 ± 40 nm) to assess their potential as new optical elements, such as a novel condenser for real-time imaging. Although the broadband light was incoherent, Supporting Information Figure S22 shows a strong interference pattern; therefore, each of the four lattice opto-materials acted as a source of coherent light. We anticipate that different combinations of lattice opto-materials will lead to the development of new imaging modalities.

In summary, we have introduced a new class of flat optics—lattice opto-materials—that use subwavelength components and an evolutionary algorithm approach to produce a large variety of far-field profiles in 3D. Lattice opto-materials can control visible light with a level of precision in 3D not possible by metalenses, plasmonic lenses, or microlenses. Furthermore, changing the size of the nanoholes allows for control of the phase of light at each lattice location, which increases both the transmission and diffraction efficiency. Anisotropic nanoholes enable the creation of lattice optics that can dynamically control the optical profile based on the polarization of light. Thus, lattice opto-materials enable opportunities for a single lattice configuration to concentrate light into different locations without physical modulation of the substrate. We anticipate that expanding the lattice units to include nanoparticles and active materials will not only increase the transmission efficiency but also enable the design of lattice opto-materials that can control the spectral distribution of transmitted light. We believe that these structured materials designed by algorithmic approaches will open new prospects for flat optics,

dx.doi.org/10.1021/nl5040573 | *Nano Lett.* 2014, 14, 7195–7200

such as integrated optoelectronic devices, aberration-free lenses, and high-resolution, 3D biological imaging.

■ ASSOCIATED CONTENT

Supporting Information

Description of the Lattice Evolution Algorithm (LEA); optimization of parameters and performance for the LEA; point-source simulation method; FDTD simulation method; confocal measurements and comparison to simulation for single focal point; FIB fabrication of lattice opto-materials; demonstration of lattice opto-materials with the same focal distance for different wavelengths; LEA for multiple focal points; comparison of simulated and measured lattice opto-materials with two focal points; comparison of simulated and measured opto-materials for 3, 5, and 7 focal points; comparison of simulated and measured lattice opto-materials with multiple phase elements; transmission spectra of gold lattice opto-materials; LEA for polarization-sensitive lattice opto-materials; bright-field and confocal measurements of compound lattice optics. This material is available free of charge via the Internet at http://pubs.acs.org.

■ AUTHOR INFORMATION

Corresponding Author

*E-mail: todom@northwestern.edu.

Author Contributions

M.D.H. developed the lattice evolutionary algorithm (LEA) method for designing the lattice opto-materials, fabricated all devices, carried out all measurements, and performed FDTD simulations of the optical responses. T.W.O. and L.J.L. guided the investigations. M.D.H. and T.W.O. analyzed the data and wrote the manuscript.

Notes

The authors declare no competing financial interest.

■ ACKNOWLEDGMENTS

This work was supported by a National Institutes of Health (NIH) Director's Pioneer Award (DP1 EB016540-05). M.D.H. was supported under Grant FA9550-05-C-0059 awarded by a Department of Defense, Air Force Office of Scientific Research, National Defense Science and Engineering Graduate Fellowship (32 CFR 168a). M.D.H. gratefully acknowledges support from the Ryan Fellowship and the Northwestern University International Institute for Nanotechnology. This work made use of the NUANCE Center facilities, which are supported by NSF-MRSEC, NSF-NSC, the Keck Foundation, the Materials Processing and Microfabrication Facility, which is supported by the MRSEC program (DMR-1121262). Computing resources were provided by the Quest high performance computing facility at Northwestern University.

■ REFERENCES

(1) Greeley, J.; Jaramillo, T. F.; Bonde, J.; Chorkendorff, I.; Norskov, J. K. *Nat. Mater.* **2006**, *5*, 909−913.
(2) Hart, G. L. W. *Nat. Mater.* **2008**, *7*, 426−427.
(3) Meredig, B.; Wolverton, C. *Nat. Mater.* **2013**, *12*, 123−127.
(4) Pendry, J. B.; Schurig, D.; Smith, D. R. *Science* **2006**, *312*, 1780−1782.
(5) Huang, F. M.; Zheludev, N. I. *Nano Lett.* **2009**, *9*, 1249−1254.
(6) Verslegers, L.; Catrysse, P. B.; Yu, Z.; White, J. S.; Barnard, E. S.; Brongersma, M. L.; Fan, S. *Nano Lett.* **2008**, *9*, 235−238.
(7) Lin, L.; Goh, X. M.; McGuinness, L. P.; Roberts, A. *Nano Lett.* **2010**, *10*, 1936−1940.
(8) Mahboub, O.; Palacios, S. C.; Genet, C.; Garcia-Vidal, F. J.; Rodrigo, S. G.; Martin-Moreno, L.; Ebbesen, T. W. *Opt. Express* **2010**, *18*, 11292−11299.
(9) Tanemura, T.; Balram, K. C.; Ly-Gagnon, D.-S.; Wahl, P.; White, J. S.; Brongersma, M. L.; Miller, D. A. B. *Nano Lett.* **2011**, *11*, 2693−2698.
(10) Soukoulis, C. M.; Wegener, M. *Science* **2010**, *330*, 1633−1634.
(11) Yu, N.; Capasso, F. *Nat. Mater.* **2014**, *13*, 139−150.
(12) Yu, N.; Genevet, P.; Kats, M. A.; Aieta, F.; Tetienne, J.-P.; Capasso, F.; Gaburro, Z. *Science* **2011**, *334*, 333−337.
(13) Jiang, Z. H.; Yun, S.; Toor, F.; Werner, D. H.; Mayer, T. S. *ACS Nano* **2011**, *5*, 4641−4647.
(14) Kern, D. J.; Werner, D. H. *Microwave Opt. Tech. Lett.* **2003**, *38*, 61−64.
(15) Chevalier, M. W.; Luebbers, R. J.; Cable, V. P. *IEEE Trans. Antennas Propag.* **1997**, *45*, 411−421.
(16) Futamata, M.; Maruyama, Y.; Ishikawa, M. *J. Phys. Chem. B* **2003**, *107*, 7607−7617.
(17) Gao, H.; Hyun, J. K.; Lee, M. H.; Yang, J.-C.; Lauhon, L. J.; Odom, T. W. *Nano Lett.* **2010**, *10*, 4111−4116.
(18) Born, M.; Wolf, E. *Principles of Optics: Electromagnetic Theory of Propagation, Interference and Diffraction of Light*, 7th ed.; Cambridge University Press: Cambridge, 1999; p 936.
(19) Davis, L. *Handbook of Genetic Algorithms*; Van Nostrand Reinhold: New York, 1991.
(20) Ishii, S.; Shalaev, V. M.; Kildishev, A. V. *Nano Lett.* **2013**, *13*, 159−163.
(21) Doucet, A.; De Freitas, N.; Gordon, N. *Sequential Monte Carlo Methods in Practice*; Springer: New York, New York, 2001.
(22) Kalyanmoy, D. *Optimization for Engineering Design: Algorithms and Examples*; Prentice Hall of India Private Limited: New Delhi, 2004; p 392.
(23) Talbot, H. F. *London Edinburgh Philos. Mag. J. Sci.* **1836**, *9*, 401−407.
(24) Yu, N.; Capasso, F. *Nat. Mater.* **2014**, *13*, 139−150.
(25) Ni, X.; Kildishev, A. V.; Shalaev, V. M. *Nat. Comm* **2013**, 4.
(26) Brolo, A. G.; McKinnon, A.; Rajora, A.; Leathem, B.; Kavanagh, K. L. *Phys. Rev. Lett.* **2004**, *92*, 037401.
(27) Chen, W. T.; Yang, K.-Y.; Wang, C.-M.; Huang, Y.-W.; Sun, G.; Chiang, I. D.; Liao, C. Y.; Hsu, W.-L.; Lin, H. T.; Sun, S.; Zhou, L.; Liu, A. Q.; Tsai, D. P. *Nano Lett.* **2014**, *14*, 225−230.
(28) Montelongo, Y.; Tenorio-Pearl, J. O.; Milne, W. I.; Wilkinson, T. D. *Nano Lett.* **2014**, *14*, 294−298.
(29) Montelongo, Y.; Tenorio-Pearl, J. O.; Williams, C.; Zhang, S.; Milne, W. I.; Wilkinson, T. D. *Proc. Natl. Acad. Sci. U.S.A.* **2014**, *111*, 12679−12683.
(30) Popovic, Z. D.; Sprague, R. A.; Connell, G. A. N. *Appl. Opt.* **1988**, *27*, 1281−1284.